CHAPTER 107

WAVE ENERGY DISSIPATION IN ROCKFILL

by

John A. McCorquodale,* MEIC, A.M.ASCE.

ABSTRACT

Wave motion in a rockfill embankment is solved by a finite element approach. Lagrangian coordinates are used to trace the movement of fluid particles on the free surface.

INTRODUCTION

Very little literature exists on the subject of unsteady non-Darcy flow in coarse granular media. However, unsteady non-Darcy flow is encountered in a few important hydraulic problems, for example,

(a) Wave absorption and transmission in rubble-mound break-waters;
(b) Water level fluctuations in the rockfill and filter zones of a dam subjected to wave action;
(c) Transmission of floods or tides through rockfill dams and causeways.

A mathematical model, to simulate the internal Darcy and/or non-Darcy flow in an embankment subjected to wave action, would permit an improved analysis of: the stability of the embankment; the stability of the armour layer; and the absorption and dissipation of wave energy by the rockfill. Since the internal flow in the embankment and the external wave action are interdependent, a complete model requires the simulation of both of these flows. Such a model would permit the computation of wave run-up and reflection. The present report is limited to the simulation of the unsteady internal flow. Heitner and Housner (4), using a finite element method, have developed an external wave action simulation for Tsunamis. The author is presently attempting to couple the internal and external models.

BACKGROUND

Experimental studies of wave absorption and transmission through rockfill models, have been reported by Johnson et al (5). The flow in their models was probably non-Darcy.

Numerous (1, 3, 7, 10, 11, 12, 13) studies have been carried out to establish the governing equations for non-Darcy flow. Saturated flow in a porous medium may be characterized (12, 13) by one of the following regimes:

(a) Microseepage (non-Newtonian flow at extremely low velocities),
(b) Darcy flow (Laminar Newtonian flow with negligible inertial effects),
(c) Non-linear laminar flow (steady streamline flow in the pores but with significant inertial effects),
(d) Turbulent transitional flow (some of the streamlines in the pores become unstable or turbulent due to inertial effects although viscous forces are still important),
(e) Fully turbulent flow (inertial effects predominate over viscous effects).

Experimental and theoretical (1, 7) studies indicate that the governing equation, for the piezometric slope, i, in steady, one-dimensional, non-Darcy flow in regimes (c) and (d), has the form

---

*Associate Professor, Department of Civil Engineering, University of Windsor, Windsor, Ontario, Canada.

$$i = |\nabla\phi| = (a + bq)q \qquad \text{.....(1)}$$

where a and b are constants for a given medium, fluid and flow regime; q = magnitude of the macroscopic or bulk velocity. The piezometric slope, for the fully turbulent regime, is described by

$$i = |\nabla\phi| = bq^2 \qquad \text{.....(2)}$$

in which $|\nabla\phi|$ = the magnitude of the piezometric gradient $\nabla\phi$.

Polubarinova-Kochina (11) gives the unsteady non-Darcy flow equation

$$i = aq + bq^2 + c\frac{\partial q}{\partial t} \qquad \text{.....(3)}$$

in which c is a constant.

The author (7) has generalized equation 3 with the limitation that the effect of convergence, divergence or curvature of the macroscopic streamlines on the conductivity is negligible; the general equation for 2 or 3 dimensional non-Darcy flow is

$$\vec{q} = -\left(\frac{1}{a+bq}\right)\left(\nabla\phi + \frac{1}{gm}\frac{\partial\vec{q}}{\partial t}\right) \qquad \text{.....(4)}$$

in which $\vec{q}$ = macroscopic velocity; g = acceleration of gravity; m = porosity.

The internal flow is subject to the continuity equation

$$\nabla\cdot\vec{q} = 0 \qquad \text{.....(5)}$$

Hence the internal governing equation is

$$\nabla\cdot\left\{\frac{1}{(a+bq)}\left[\nabla\phi + \frac{1}{gm}\frac{\partial\vec{q}}{\partial t}\right]\right\} = 0 \qquad \text{.....(6)}$$

Equation 6 is to be solved for $\phi = \phi(x,y,t)$ within a time varying solution domain, subject to a set of initial conditions and certain time dependent (periodic) boundary conditions (see figure 1). An important aspect of the wave action problem is the determination of the phreatic surface (in the rockfill) as a function of time.

Lean (6) has solved the problem of wave action in a highly permeable wave absorber by invoking the Dupuit assumption to obtain the following equations for the wave motion:

$$\frac{\partial\eta}{\partial t} = -\frac{\partial(h_o u)}{\partial x} \qquad \text{.....(7)}$$

$$\frac{\partial u}{\partial t} = -g\frac{\partial\eta}{\partial x} - \frac{ku|u|}{h_o} \qquad \text{.....(8)}$$

where the variables are defined in figure 2.

Equations 7 and 8 were solved analytically by linearizing the friction term.

Another possible method of solution (2, 7) which has been developed by M. S. Nasser at the University of Windsor, is the method of characteristics; however in order to obtain a practical formulation of the problem, it is again necessary to

use the Dupuit assumption. The characteristic solution can be developed from

$$\begin{bmatrix} (h_o + \eta)/m & 0 & u/m & 1 \\ u/m & 1 & gm & 0 \\ dx & dt & 0 & 0 \\ 0 & 0 & dx & dt \end{bmatrix} \begin{Bmatrix} \frac{\partial u}{\partial x} \\ \frac{\partial u}{\partial t} \\ \frac{\partial \eta}{\partial x} \\ \frac{\partial \eta}{\partial t} \end{Bmatrix} = \begin{Bmatrix} 0 \\ -gm\,F(u)\,u \\ du \\ d\eta \end{Bmatrix} \qquad \text{.....(9)}$$

in which $F(u) = a + b|u|$.

Lean's method and the method of characteristics are useful for and applicable to the case in which the inertial effects are large compared with the friction effects. However, in the case of unsteady flow through sand and gravel embankments the friction effects predominate over the inertial effects and often the Dupuit assumption is not justified because of the two dimensional nature of the flow. The method described in this paper is applicable to the latter case.

MATHEMATICAL FORMULATION

Simplified Equations

If the inertial term, $(1/gm)\partial\vec{q}/\partial t$, in Eq. 6, is small compared to $|\nabla\phi|$ and has nearly the same line of action as $\nabla\phi$ and $\vec{q}$, then the transformation

$$\nabla\zeta = \nabla\phi + \frac{1}{gm}\frac{\partial\vec{q}}{\partial t} \qquad \text{.....(10)}$$

can be introduced in order to reduce Eq. 6 to

$$\nabla.\{K(|\nabla\zeta|)\nabla\zeta\} = 0 \qquad \text{.....(11)}$$

The macro-velocity is now approximated by

$$\vec{q} = -K(|\nabla\zeta|)\nabla\zeta \qquad \text{.....(12)}$$

in which $K(|\nabla\zeta|) = \frac{a}{2b}\left\{\frac{\sqrt{1 + c|\nabla\zeta|} - 1}{|\nabla\zeta|}\right\}$ .....(13)

and $c = 4b/a^2$.

The variational form of Eq. 11 is, (7,8,9),

$$\delta\chi = \int_{t_o}^{t}\int_{A(\tau)} \delta[K(|\nabla\zeta|)(|\nabla\zeta|)^2 + G(|\nabla\zeta|)]\,dA\,d\tau = 0 \qquad \text{.....(14)}$$

in which t_o = initial time;

$$G(|\nabla\zeta|) = \frac{a}{6bc}(2 - c|\nabla\zeta|)\sqrt{1 + c|\nabla\zeta|} \qquad \text{.....(15)}$$

$A(\tau)$ = solution domain.

The boundary conditions for the transformed variable ζ are (see figure 3):

(a) on E A B :- $\frac{\partial\phi}{\partial n} = 0$ and $\frac{\partial\zeta}{\partial n} = 0$;

(b) on E D :- $\phi \simeq y_D$ and $\frac{\partial\phi}{\partial y} \simeq 0$ and

$\zeta \simeq \phi$ and $\frac{\partial\zeta}{\partial y} \simeq 0$;

(c) on D C :- $\phi \simeq y \simeq \zeta$;

(d) on C B :- $\phi = y$; ζ is found from Equation 10; a particle on the free surface remains on the free surface.

Within the approximation of the original transformation, the transformed boundary conditions satisfy the self-adjoint requirement for the variational format.

THE FINITE ELEMENT MODEL

The finite element method is useful for solving free surface problems because of the ease with which certain boundary conditions and variable geometry can be met. The solution domain, A(t), can be discretized by elements of the type shown in figure 4. Figure 3 shows a typical discretization at an instant in time.

The variation of ζ within each element is assumed to be

$$\zeta^e = (\beta_1 + \beta_2 x + \beta_3 y)t + \beta_4 + \beta_5 x + \beta_6 y \qquad \text{.....(16)}$$

where β_i are defined in terms of the six nodal conditions on ζ, x, y and t; thus for $0 \leqslant t \leqslant \Delta t$

$$\begin{Bmatrix} \beta_4 \\ \beta_5 \\ \beta_6 \end{Bmatrix} = \begin{bmatrix} 1 & x_\ell & y_\ell \\ 1 & x_m & y_m \\ 1 & x_n & y_n \end{bmatrix}^{-1} \begin{Bmatrix} \zeta_\ell \\ \zeta_m \\ \zeta_n \end{Bmatrix} \qquad \text{.....(17)}$$

and

$$\begin{Bmatrix} \beta_1 \\ \beta_2 \\ \beta_3 \end{Bmatrix} = [(\Delta t)^{-1}] \begin{bmatrix} 1 & x_i & y_i \\ 1 & x_m & y_m \\ 1 & x_k & y_k \end{bmatrix}^{-1} \begin{Bmatrix} \Delta\zeta_i \\ \Delta\zeta_j \\ \Delta\zeta_k \end{Bmatrix} \qquad \text{.....(18)}$$

in which

$$\Delta\zeta_i = \zeta_i - (\beta_4 + \beta_5 x_i + \beta_6 y_i) \qquad \text{.....(19)}$$

is the change in ζ_i during an interval Δt.

The finite element equivalent of Eq. 14 is

$$\frac{\partial \hat{\chi}}{\partial \zeta_i} = \Sigma \frac{\partial \hat{\chi}^e}{\partial \zeta_i} = 0 \qquad \text{.....(20)}$$

where

$$\frac{\partial \hat{\chi}^e}{\partial \zeta_i} = \int_o^{\Delta t} \int_{A(t)^e} \{\frac{\partial}{\partial \zeta_i} [K(|\nabla \zeta^e|)(|\nabla \zeta^e|)^2 + G(|\nabla \zeta^e|)]\} \, dAdt \qquad \text{.....(21)}$$

Substituting from Eq. 16 for ζ^e yields, after integration

$$\sum_{j=i}^{k} \sum_{e=1}^{N} \frac{\bar{K}^e \bar{A}^e}{A_1^e} [3(\beta_5 b_i + \beta_6 c_i)^e + S_{ij}^e \Delta\zeta_j] = 0 \qquad \text{.....(22)}$$

in which $\bar{K}^e = (K^e_{t=o} + K^e_{t=\Delta t})/2$;

$\bar{A}^e = (A_1^e + A_2^e)/2$;

A_1^e = area of triangle ijk;

A_2^e = area of triangle ℓmn;

$S_{ij} = (b_i b_j + c_i c_j)/A_1^e$;

$b_i = y_j - y_k$;

$c_i = x_k - x_j$;

N = number of elements.

CALCULATION OF THE FREE SURFACE MOVEMENT

The position of the free surface after a time increment Δt can be found from

$$\vec{s}(X,Y,\Delta t) = \vec{\bar{q}}\Delta t/m + \vec{s}(X,Y,O) \qquad \text{.....(23)}$$

where $\vec{s}(X,Y,t)$ = position of a free surface particle at time t (lagrangian form); $\vec{\bar{q}}$ = average 'bulk' velocity of the surface particle for the interval Δt (see figure 5). Since $\vec{\bar{q}}$ depends to some extent on the new free surface position, the computation of $\vec{\bar{q}}$ must be obtained by an iterative of trial and error process. Eq. 23 was also utilized to predict the motion or the outcrop point, C. The coordinates of the internal nodes of the elements must be adjusted as the free surface moves.

At each time step, Δt, a new free surface ϕ is computed from $\phi = y + C$; Eq. 10 is used to obtain the corresponding ζ. A transformation is obtained by integrating Eq. 10 along a streamtube to yield approximately

$$\zeta = \phi + \frac{1}{gm} \overline{\left(\frac{\partial q}{\partial t}\right)} S_p \qquad \text{.....(24)}$$

in which $\overline{(\partial q/\partial t)}$ is a representative average value of $\partial \vec{q}/\partial t$ along the streamtube, and S_p is the length of the streamtube. Since the inertia term is assumed to be small compared with friction, the values for S_p can be estimated on the basis of a solution in which $\zeta \equiv \phi$.

JUSTIFICATION OF ASSUMPTIONS

A one dimensional solution of Equation 6, for accelerating flow in a typical gravel, (8), indicates that the time required to reach 90% of the terminal (friction) velocity, corresponding to i = 1, is given by

$$t \simeq \frac{0.1}{gmb} \qquad \text{.....(25)}$$

or approximately .06 seconds for 4.4 cm crushed rock. With zero applied piezometric gradient, the maximum terminal velocity will decay to 10% of its value in

$$t \simeq \frac{.6}{gmb} \qquad \text{.....(26)}$$

or 0.4 seconds for 4.4 cm rock which corresponds to a particle displacement of about one grain diameter.

The case of rapid drawdown in a rockfill has been solved using Equation 6 without the inertia term (9), and with the inertia term (8). The results of these studies are summarized and compared with experimental results in figure 6. It is noted that the effect of the inertia term is small (as assumed in this paper) and that the numerical results are in agreement with the experimental results.

NUMERICAL ANALYSIS

Equations 22 and 23 were utilized to simulate wave motion in an embankment of 4.4 cm crushed rock ($a = .005$ sec/cm; $b = .004$ sec^2/cm^2; $m = 0.40$), as shown in figure 3. The right hand rockface is subjected to a periodic hydrostatic force produced by varying the external water depth according to

$$y_D = \bar{y}_o - A_o \sin\left(\frac{2\pi t}{T}\right)$$

in which $\bar{y}_o$ = mean tail water level (56 cm); T = wave period (2π seconds); A_o = wave amplitude outside rockfill (20 cm). The initial condition is $h_o = \bar{y}_o$ = 56 cm.

It is assumed that the internal free surface level at C will always be equal or higher than y_D.

The solution of Equation 22 and 23 is summarized in the flowchart, figure 7. Equation 22 was linearized and solved by successive over-relaxation (SOR factor = 1.65) at each time step ($0.05 < \Delta t < .2$ sec). In order to start the solution of Eq. 22 the free surface DB at the end of interval Δt is initially assumed to be the same as at the beginning of Δt; on this basis the necessary surface velocities for the application of Eq. 23 are obtained and hence a new free surface can be estimated.

As figure 7 indicates, this approximate solution is 're-cycled' to correct for non-linearities in the system and thus to improve the solution. The computation at a particular time step is complete when successive estimates of the free surface are within a specified tolerance.

The computations were carried out on an IBM 360/40 computer. A typical computer solution for the wave action on certain selected points is shown in figure 8. About 10 minutes of computer time was required for this solution.

EXPERIMENTAL VERIFICATION

Experimental studies, using a wave flume, are now under way to test the proposed numerical simulation. Figure 9 compares the predicted and preliminary experimental wave transmission curve, for a 4.4 cm rock embankment.

CONCLUSIONS

The proposed finite element model for unsteady non-Darcy flow is developed for the case when the influence of $(1/gm)\partial q/\partial t$ is small compared to the influence of turbulence. The available experimental studies appear to indicate that the proposed model is valid for unsteady flow in rockfill for rock sizes up to about 4 cm.

LIST OF REFERENCES

1. Ahmed, N., and Sunada, D. K., 'Nonlinear Flow in Porous Media', Journal of the Hydraulic Division, ASCE, Vol. 95, HY6, Nov. 1969.
2. Dracos, T., 'Calculation of the Movement of the Outcrop Point', Proc. XIII, Congress of the IAHR, Paper D-2, Kyoto, Japan, 1969.
3. Dudgeon, C. R., 'Flow of Water Through Coarse Granular Materials', Master of Engineering Thesis, University of New South Wales, 1964.
4. Heitner, K. L., and Housner, G. W., 'Numerical Model for Tsunamic Run-up', Journal of the Waterways and Harbour Division, ASCE, Vol. 96, WW3, August 1970.
5. Johnson, J. W., Kondo, H., and Wallihan, R., 'Scale Effects in Wave Action Through Porous Structures', Proc. 10th Conference on Coastal Engrg, Tokyo, 1966.
6. Lean, G. H., 'A Simplified Theory of Permeable Wave Absorbers', J. of Hydraulic Research, Vol. 5, No. 1, 1967.
7. McCorquodale, J. A., 'Finite Element Analysis of non-Darcy Flow', Ph.D. Thesis, Department of Civil Engineering, University of Windsor, Canada, 1970.
8. McCorquodale, J. A., 'The Finite Element Method Applied to Unsteady non-Darcy Flow', 18th Annual Special Conference, Hydraulics Division, ASCE, University of Minnesota, 1970.
9. McCorquodale, J. A., 'A Variational Approach to non-Darcy Flow', Journal of the Hydraulics Division, ASCE, Vol. 96, HY11, Nov. 1970.
10. Nasser, M. S. 'Radial non-Darcy Flow Through Porous Media', M.A.Sc. Thesis, Department of Civil Engineering, University of Windsor, 1970.
11. Scheidegger, A. E. ed., 'The Physics of Flow through Porous Media', 2nd ed., University of Toronto Press, Toronto, Canada, 1960.
12. Ward, J. C., 'Turbulent Flow in Porous Media', Journal of the Hydraulics Division, ASCE, Vol. 90, HY5, Sept. 1964.
13. Wright, D. E. 'Nonlinear Flow Through Granular Media', Journal of the Hydraulics Division, ASCE, Vol. 94, HY4, July 1968.

LIST OF SYMBOLS

a	=	a constant;
A	=	area;
A^e	=	area of an element;
A_o	=	wave amplitude;
b	=	a constant;
b_i	=	$y_j - y_k$;
c	=	a constant;
c_i	=	$x_k - x_j$;
e	-	superscript indicates element;
g	=	acceleration due to gravity;
h_o	=	depth measured from the initial mean water level;
i	=	slope of the piezometric grade line;
$\left.\begin{matrix} i,j,k \\ l,m,n \end{matrix}\right\}$	-	indices;
k	=	constant;
$K(-)$	=	hydraulic conductivity;
m	=	porosity;
$\vec{q}$	=	macroscopic velocity;
$s(X,Y,t)$	-	Lagrangian coordinates;
S_{ij}	=	$(b_i b_j + c_i c_j)/A_l^e$;
S_p	=	streamtube length;
t	=	time;
T	=	period;
u	=	horizontal component of velocity;
(x,y,z)	-	Cartesian coordinates;
y_o	=	mean tailwater depth;
β_i	-	coefficients in the elemental representation of ζ^e ;
η	=	height of perturbation measured from initial mean W-L;
ϕ	=	piezometric head;
χ	=	functional;
ζ	=	transformed dependent variable.

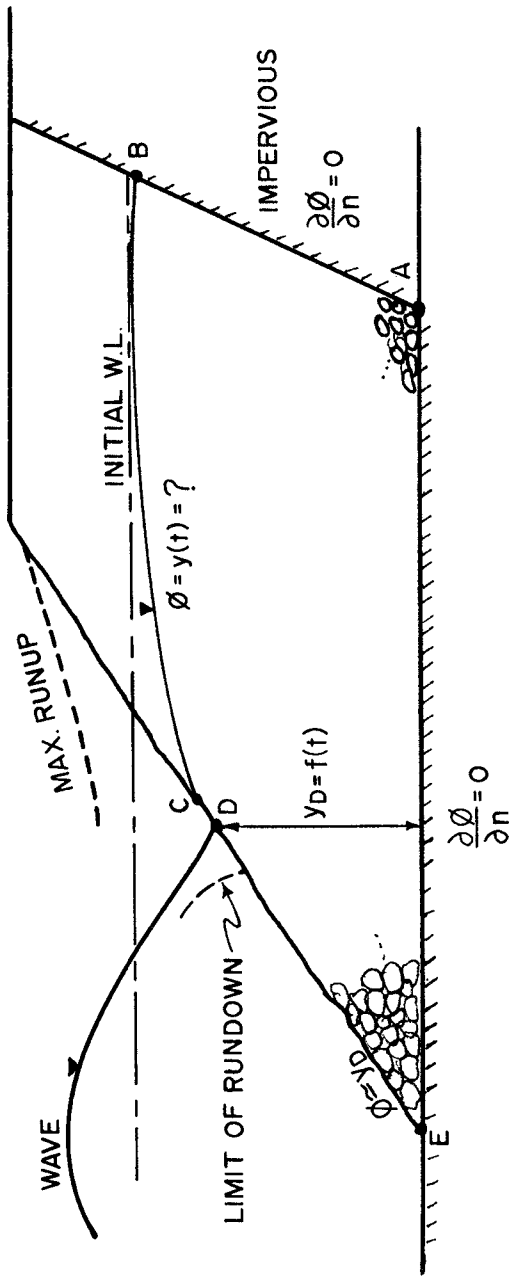

FIGURE 1 Typical Unsteady Non-Darcy Flow Problem.

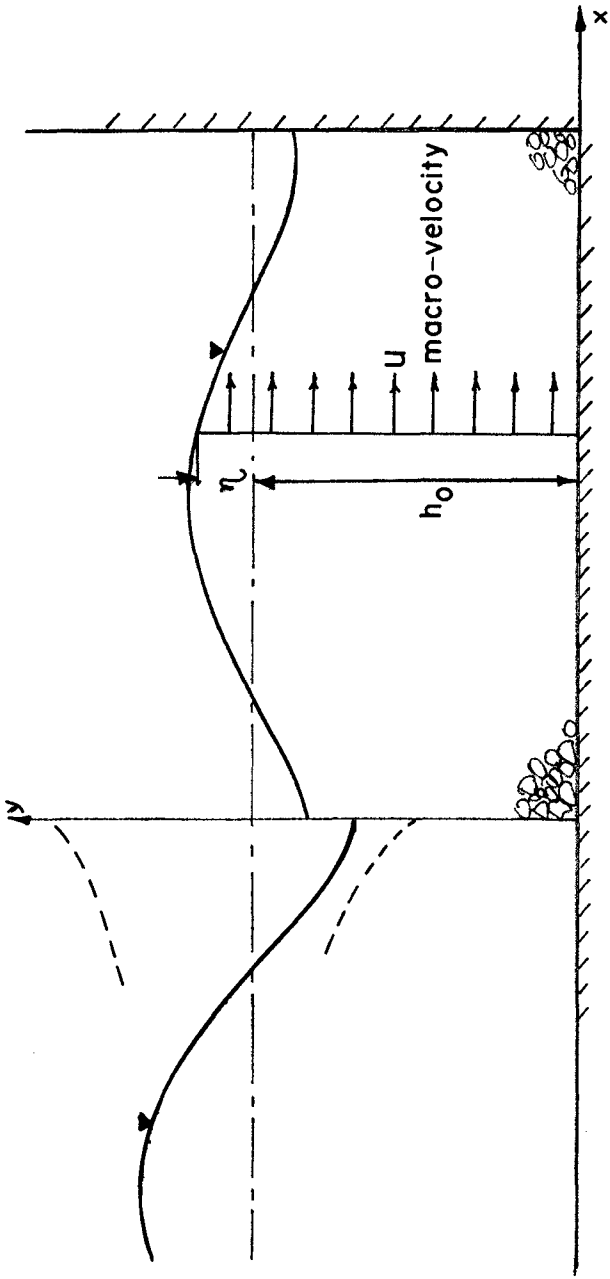

FIGURE 2 Defining Diagram.

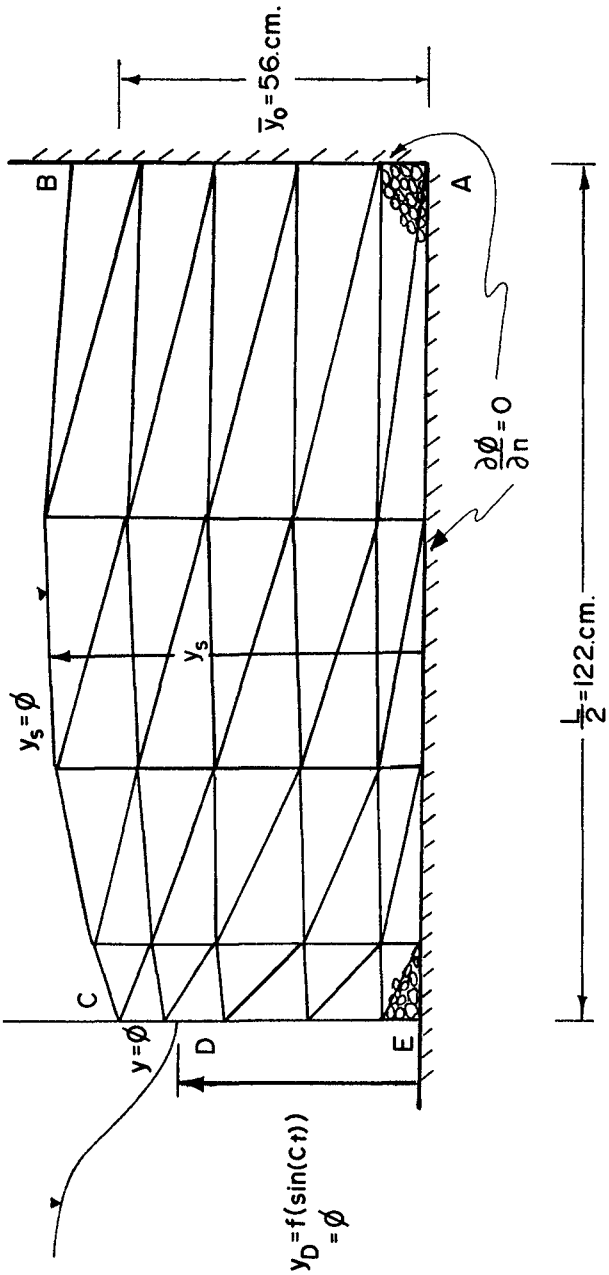

FIGURE 3 Boundary Conditions and Finite Element Discretization for the Illustrative Non-Darcy Flow Problem.

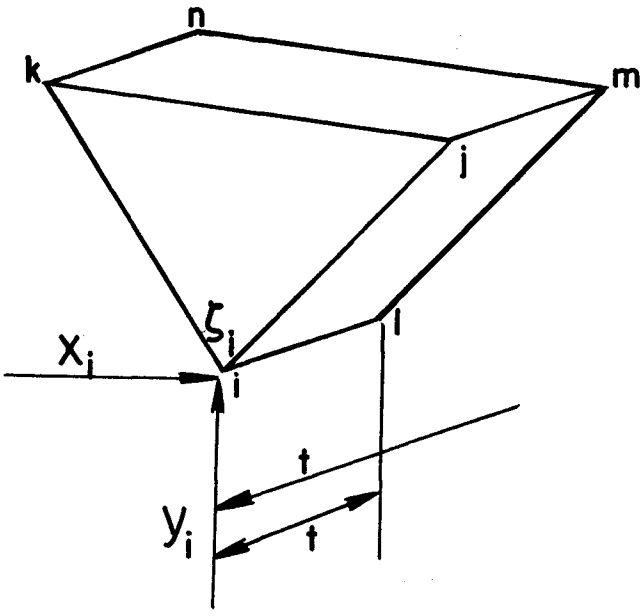

FIGURE 4 Typical Element in (x-y-t) Space.

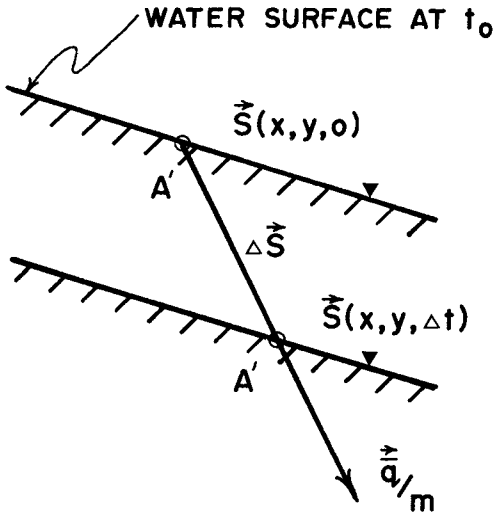

FIGURE 5 Lagrangian Approach to Tracing Particles on the Free Surface.

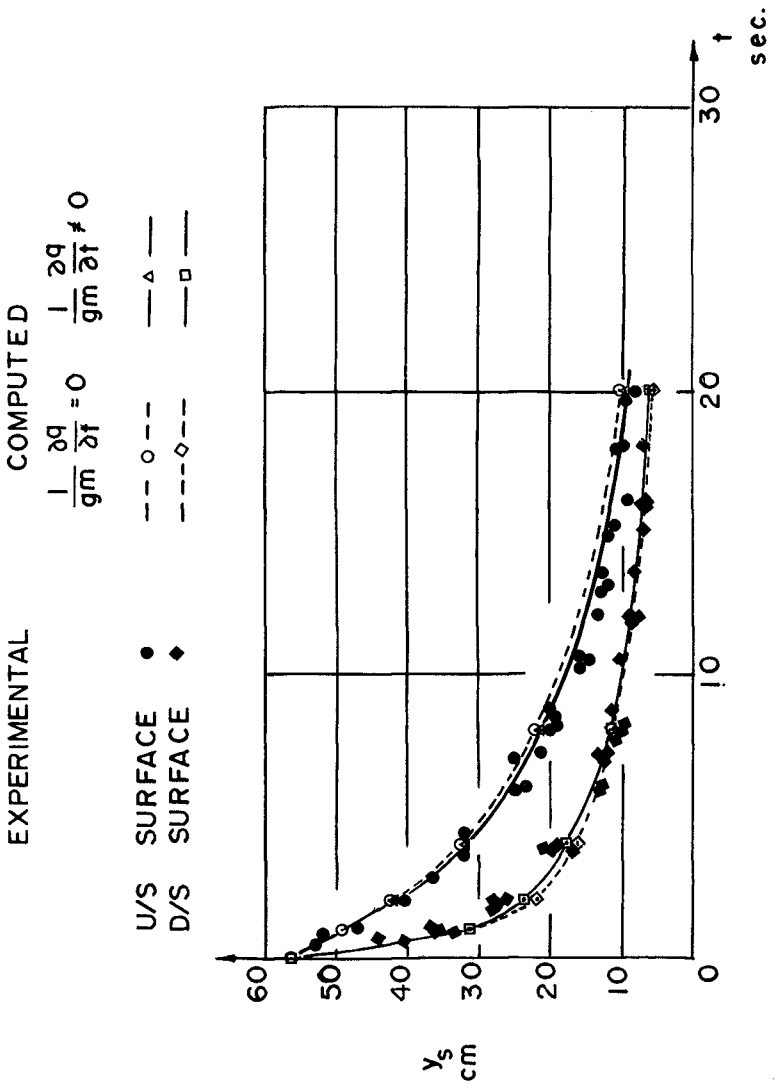

FIGURE 6 Experimental and Numerical Recession Curves for Rapid Drawdown in a Crushed Rock Embankment (4.4 cm. Rock).

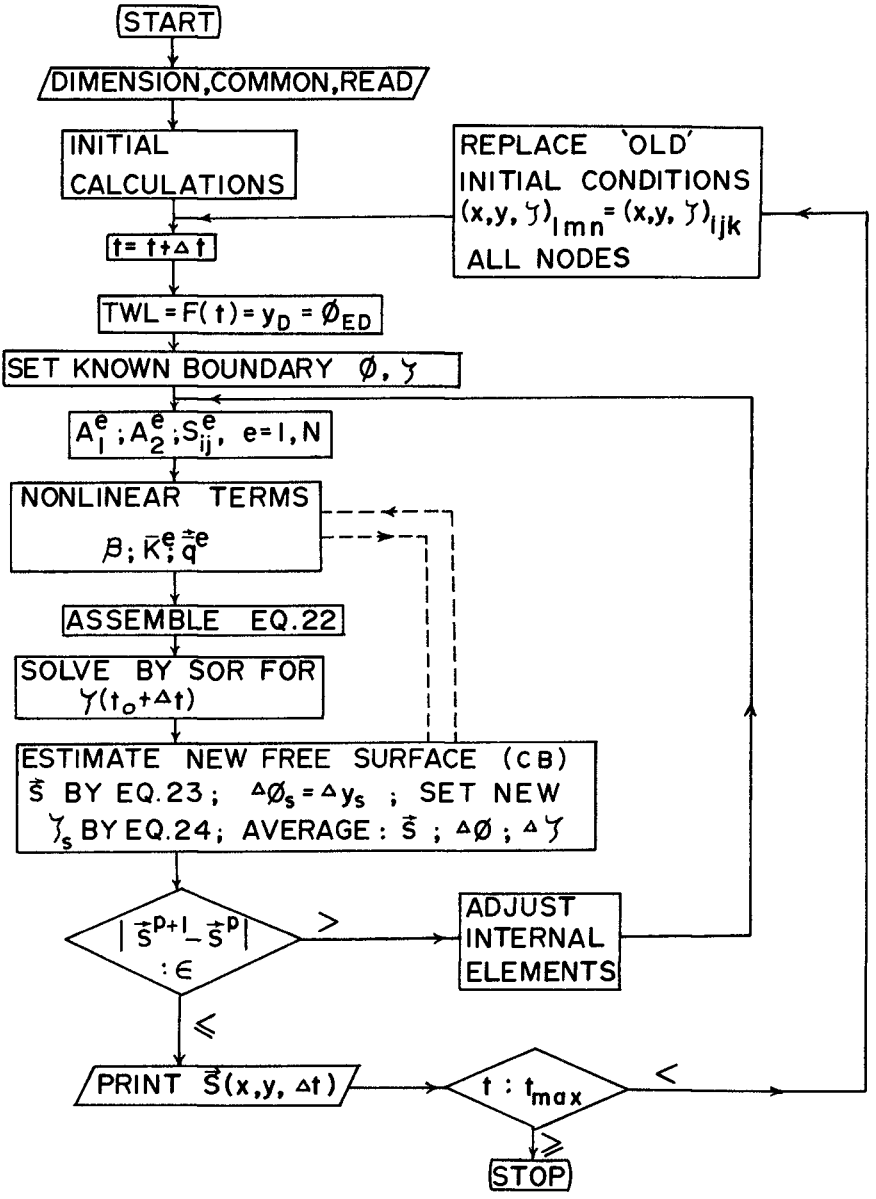

FIGURE 7 Computer Flow Chart.

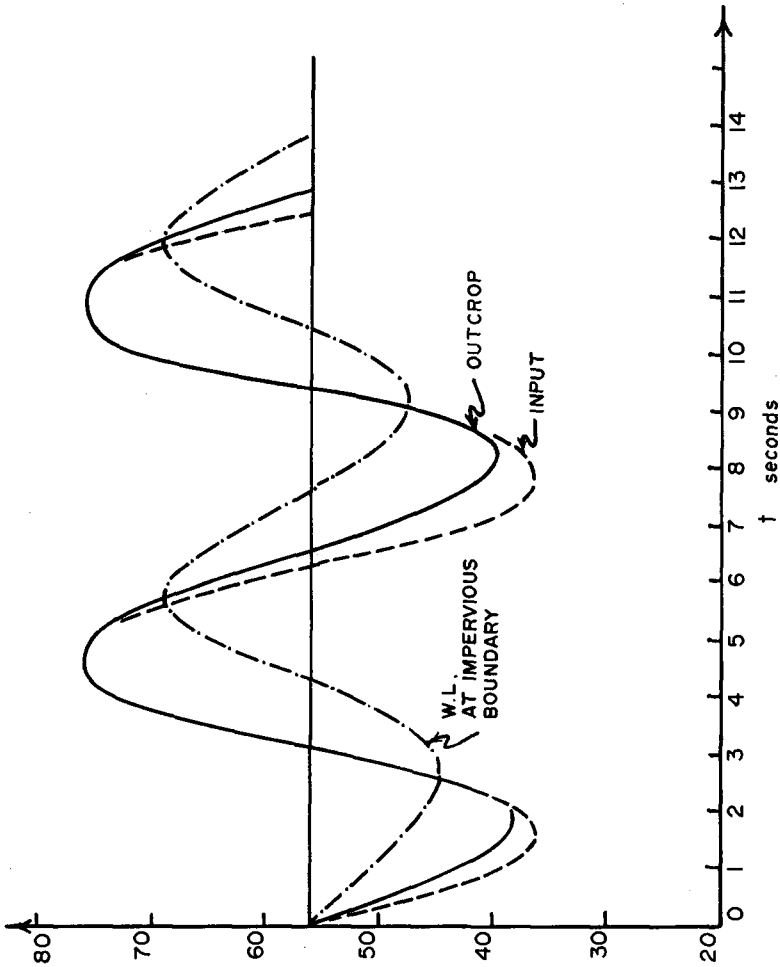

FIGURE 8 Computed Wave Motions at Selected Verticals.

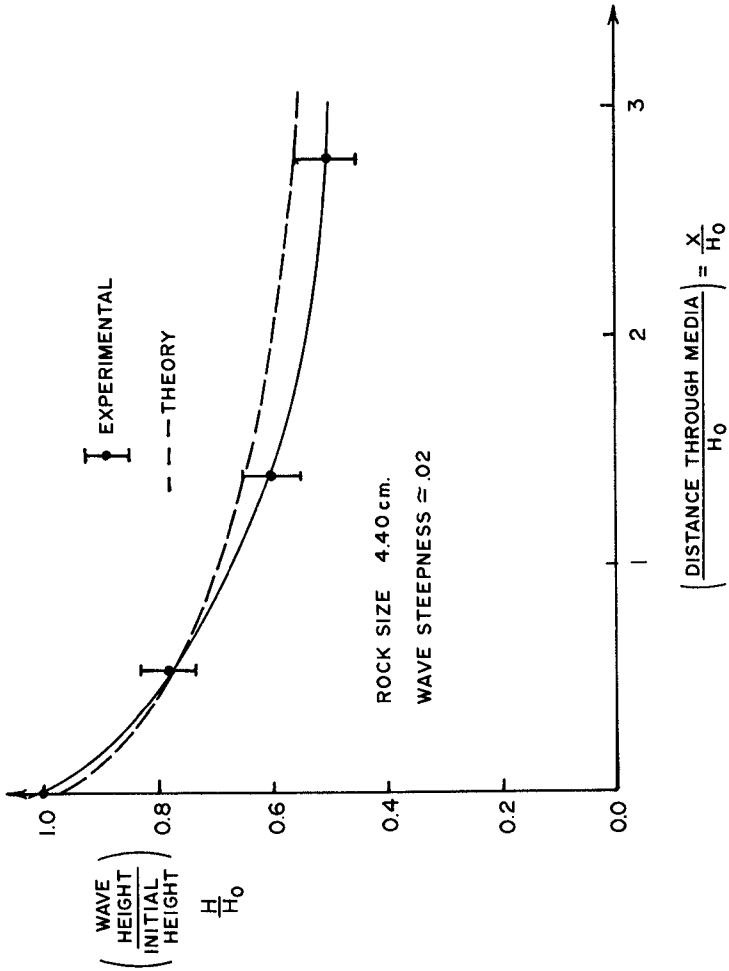

FIGURE 9 Computed and Preliminary Experimental Wave Transmission Curves for 4.4 cm. Crushed Rock.